Vibration characteristics measurement of beam-like structures using infrared thermography

S.M. Talai [a,1], D.A. Desai [a], P.S. Heyns [b]

[a]*Sound & Vibration Group, Tshwane University of Technology, Private Bag X680, Pretoria 0001, South Africa*
[b]*Centre for Asset Integrity Management, University of Pretoria, Private Bag X20, Hatfield 0028, South Africa*

HIGHLIGHTS

- A new IRT technique developed for structural vibration measurement in terms of frequency and displacement
- Frictional temperature evolution obeys coulomb law of friction
- Frictional heat generation increases with structural excitation frequency
- FFT checks the spectral peak in the noisy DFT temperature signature
- Heat transfer in the beam through conduction is non-linear, thus, finite temperature equation is used for computation of structural displacement

Keywords:
Vibration behaviour
Infrared thermography
Frictional heat generation
Condition monitoring

ABSTRACT

Infrared thermography (IRT) has matured and is now widely accepted as a condition monitoring tool where temperature is measured in a non-contact way. Since the late 1970s, it has been extensively used in vibrothermography (Sonic IR) non-destructive technique for the evaluation of surface cracks through the observation of thermal imaging of the vibration-induced crack heat generation. However, it has not received research attention on prediction of structural vibration behaviour, hence; the concept to date is not understood. Therefore, this paper explores its ability to fill the existing knowledge gap. To achieve this, two cantilever beam-like structures couple with a friction rod subjected to a forced excitations while infrared cameras capturing the thermal images on the friction interfaces. The analysed frictional temperature evolution using the Matlab Fast Fourier Transform (FFT) algorithm and the use of the heat conduction equation in conjunction with a finite difference approach successfully identifies the structural vibration characteristics; with maximum error of 0.28 % and 20.71 % for frequencies and displacements, respectively. These findings are particularly useful in overcoming many limitations inherent in some of the current vibration measuring techniques applied in structural integrity management such as strain gauge failures due to fatigue.

[1] Corresponding author. Address: Department of Mechanical Engineering, Mechatronics & Industrial Design; Tshwane University of Technology, Private Bag X680, Pretoria 0001, South Africa; E-mail address: TalaiSM@tut.ac.za

1. Introduction

The structural integrity of mechanical dynamic structures is the key to its successful operation [1-5]. The available literature indicates that, condition monitoring of vibrating structures has long been an active area of research since 1950s; when Arthur Crawford first acknowledged the challenge to acquire an effective way for structural vibration analysis. To date, the interest seems to be centred towards an effective real time techniques. The direct methods of measurements such as strain gauges have predominantly been used to monitor the potential structural vibration. Although they have the advantage of performing measurement of an individual structure, it has several disadvantages such as; shorter sensor life span due to continued cyclic loading; leading to failure by fatigue [6].

However, Infrared thermography (IRT) has been greatly applied to the vibrothermography non-destructive technique where the surface cracks are evaluated through the observation of thermal imaging of vibration-induced heat generation. Recent studies have shown that defect heating in cracked metallic structure is primarily generated by frictional rubbing on crack faces [7]. Mabrouki et al. [8] investigated the vibrothermography for detection of fatigue cracks in steel compact tension specimen. Lahiri et al. [9] proposed the active IRT based technique for detecting defects in ferromagnetic specimens using low frequency alternating magnetic field induced heating. The authors observed an increase in the surface temperature using an infrared camera due to induced eddy current leading to joule heating. Furthermore, Montanini and Freni [10] established that there exists a correlation of vibrational mode shape to viscoelastic heat generation in vibrothermography. Therefore, analysis of frictional heat generation due to interacting components can result to a quick and reliable indication of the structural vibration characteristics.

On the other hand, friction is often considered by engineers as detrimental to the design of dynamic mechanisms involving mating parts. Nonetheless, it has long been established that it can as well provide a very effective means of dissipating vibratory energy in elastic structures. This technique is in applications such as turbomachinery bladed disks, where either the lacing wire is incorporated at the chosen location of the blade structure or direct interaction of the constitutive blades through shrouded tip approach for enhancing passive dissipation of vibratory energy [11]. In reality, it is often structural joints that are more responsible for energy dissipation than the (solid) material itself [12, 13]. Ultimately, this leads to temperature increase at the contact interface [14].

Despite the large amount of research conducted on condition monitoring using infrared thermography as indicated in the recent comprehensive literature review by Bagavathiappan et al. [15], no research attention has been paid to the investigation of its application to the vibration measurement. Furthermore, Dimarogonas and Syrimbeis [16] successfully studied the thermal signature of a vibrating plate due to material damping. However, no further work has been done. Hence; to date the concept is not understood even though IRT has matured and widely accepted as a condition monitoring tool where temperature is measured in a non-contact way.

Therefore, it was the aim of this study to investigate experimentally the ability of using IRT in vibration measurement. This will go a long way to saving the industries from the expensive down time in stopping the process to diagnose the potential structural malfunctioning through vibration. Nevertheless, it is important to mention that friction is a complex phenomenon due to its nonlinearity [17]. However, the difficulty lies in relating frictional thermal signatures to vibration behaviour. Hence, in order to explore this, this study employs two cantilever beam-like structures coupled with a slipping friction rod for its analysis. The frequency and transverse displacement parameters of vibration characteristics are considered in this paper.

The electrodynamic modal shaker utilised for the mechanical excitations, while infrared cameras focused on the beam-friction rod interfaces. Further, the results are validated against attached accelerometer acquired measurements.

The methodology developed forms the basis for online structural vibration monitoring employing IRT. Its benefit to the maintenance

is the ability of using a single diagnostic tool for dual condition monitoring *(vibration and thermal distribution).* In addition, it has the great potential of overcoming many limitations experienced with current condition monitoring techniques such as strain gages failure due to fatigue, including being employed in a remote and hostile environment; whereas the other available techniques may be inappropriate.

2. Mathematical model of correlation of beam transverse displacement to surface frictional temperature distribution

The heat conduction equation for the Cartesian co-ordinate system (x, y, z) on the blade surface differential element can be expressed as [18]

$$\frac{\partial^2\theta}{\partial x^2}+\frac{\partial^2\theta}{\partial y^2}+\frac{\partial^2\theta}{\partial z^2}+\frac{q_g}{k}=\frac{1}{\alpha}\frac{\partial\theta}{\partial t} \quad (1)$$

where θ is the temperature rise on the beam surface, k is the thermal conductivity, ρ is the material density and c is the specific heat capacity, q_g is the heat generated per unit volume and α is the thermal diffusivity. The grid distribution technique as given in Fig. 1 analyses the surface temperature. Making the following assumptions:

i. Temperature has reached a steady state condition
ii. The beam is thin, hence the temperature distribution is uniform along the thickness
iii. Heat lost through forced convection was $30\ W/m^2.K$ at $22\ ℃$ [19]. It obeys the Newton's law of cooling $(q = h_{con}\theta)$ and is the heat lost on both sides of the beam. However, heat lost by radiation is ignored since its negligible compared to the heat lost through forced convection [16]

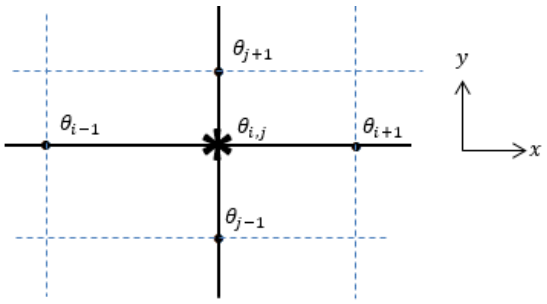

Fig. 1. Finite surface temperature distribution grid.

Thus, the temperature rise finite difference equations for the grid in Δx and Δy are

$$\frac{\partial^2\theta}{\partial x^2}=\frac{1}{(\Delta x)^2}\left(\theta_{i+1}-2\theta_{i,j}+\theta_{i-1}\right),$$

$$\frac{\partial^2\theta}{\partial y^2}=\frac{1}{(\Delta y)^2}\left(\theta_{j+1}-2\theta_{i,j}+\theta_{j-1}\right) \quad (2)$$

Substituting Eq. (2) into Eq. (1), the heat distribution in terms of temperature finite differences developed

$$q_g(x,y)=k\left[\frac{2h_{con}}{ck}\theta_{i,j}-\frac{\partial^2\theta}{\partial x^2}-\frac{\partial^2\theta}{\partial y^2}\right] \quad (3)$$

Considering a sinusoidal force for the beams excitation, the steady state displacement response can be given by [20]

$$z(t)=Zsin(\omega t) \quad (4)$$

where Z is the amplitude and ω is the excitation frequency. The frictional heat generation, q_g per half a cycle is $2\mu NfZ$ [21], so that

$$q_g=\frac{2\mu Nfz(t)}{sin(\omega t)} \quad (5)$$

In order to obtain the structural displacement equation from the acquired thermal imager, the beam surface temperature is equated to the frictional heat evaluation. Therefore, comparing Eq. (3) and (5), the equation of structural transverse displacement is developed

$$z(t) = \frac{ksin(\omega t)}{2\mu N\omega}\left[\frac{2h_{con}}{ck}\theta_{i,j} - \frac{\partial^2\theta}{\partial x^2} - \frac{\partial^2\theta}{\partial y^2}\right] \quad (6)$$

Eq. (6) is allows the computation of the beam transverse displacement from the analysis of the thermal imager surface temperature distribution.

3. Materials and experimental method

3.1. Materials

In the present study, both the beam and friction rod were manufactured of AISI 304 stainless steel. The choice based on the ability to generate heat with slight frictional effect. Typically, they have low thermal conductivity [8]. The geometric and material properties are given in Table 1 and Table 2, respectively.

Table 1
Beam and friction rod geometric dimensions.

Description	Dimension
Beam mass	0.10 kg
Length	300 mm
Width	25 mm
Thickness	2 mm
Friction rod diameter	5 mm
Beam hole diameter [21] [tolerance grade: $F8/js7$]	$5^{+0.422}_{+0.412}$ mm
Beam-friction rod hole location from fixed end	250 mm
Location of the exciters	290 mm

Table 2
Material properties for the AISI 304 steel [22].

Material properties	Parameters
Density, ρ	7740 kg/m^3
Young modulus, E	200 GPa
Poisson ratio,ν	0.33
Static friction coefficient, μ_s ($\mu_k = 0.75\ \mu_s$) [23]	0.15
Thermal material properties	
Thermal conductivity, k	16.5 W/mK
Specific heat capacity, c	500 J/kgK

3.2. Experimental procedure

A suitable manufactured rig, fixed the beams and friction rod as required. The laboratory experimental setup was as presented in Fig. 2. Two infrared cameras were used. The Micro-epsilon TIM160 infrared camera focused on the friction interface of beam 1. It has a thermal sensitivity of 80 mK, spectral range of 7.5 - 13 μm, optical resolution of 160 × 120 Pixels, frame rate real time of 120 Hz and lenses FOV of 23 °. On the hand, Flir A325sc infrared camera focused on the friction interface of beam 2. It has a thermal sensitivity of 50 mK, spectral range of 7.5 -13μm, optical resolution of 320 × 240 Pixels, frame rate real time of 60 Hz and lenses FOV of 25 °.

Spider box X80 vibration controller *(operated by PC 2)* firstly, generated the required signals through the output 1 and 2 for vibration shaker attached to beam 1*(Brüel & Kjær, model 4824)* and beam 2 *(Sentek, model MS-1000)*, respectively. The signal for the former was amplified by Brüel & Kjær, model 2732 amplifier while the latter by Sentek, model LA 1500 amplifier. These facilitated the beams mechanical excitation. Secondly, controlled the vibration excitation via channel 1 by a miniature Deltatron accelerometer type 4507 *(sensitivity of 9.989 mV/ms^{-2})* attached to beam 1 for closed loop operation, thus, protecting the shakers against the sudden overloads. Thirdly, recorded the beam dynamic responses through channel 2 and 6 via miniature Deltatron accelerometers type 4507 *(sensitivity of 1.025 mV/ms^{-2})* attached to beam 1 and 2, respectively *(attached at 2 mm from the interface and opposite side of the zone under focus by an IR camera to avoid interference of thermal recording)*. The aim of this was for validation of vibration parameters predicted using IRT approach. Finally, recorded the friction interface pre-load and dynamic force through channel 5 via a load cell (HMB) with a rated sensitivity of 20 mV/N.

Furthermore, the problem of low thermal emissivity of the beams surfaces was eliminated by applying black paint which is consistent with standard practice [8].

The two sets of experiments were carried out. Firstly exciting both beams at 20 Hz. Secondly exciting beam 1 at 40 Hz and beam 2 at 20 Hz. The excitation frequencies were

considered based on the sampling rule of 2.5 times the sampling rate in relation to the rated optical resolution of the IR cameras used. During the entire excitation period, the thermal images were recorded continuously for 150 s and the images stored in the PC 1 for post analysis.

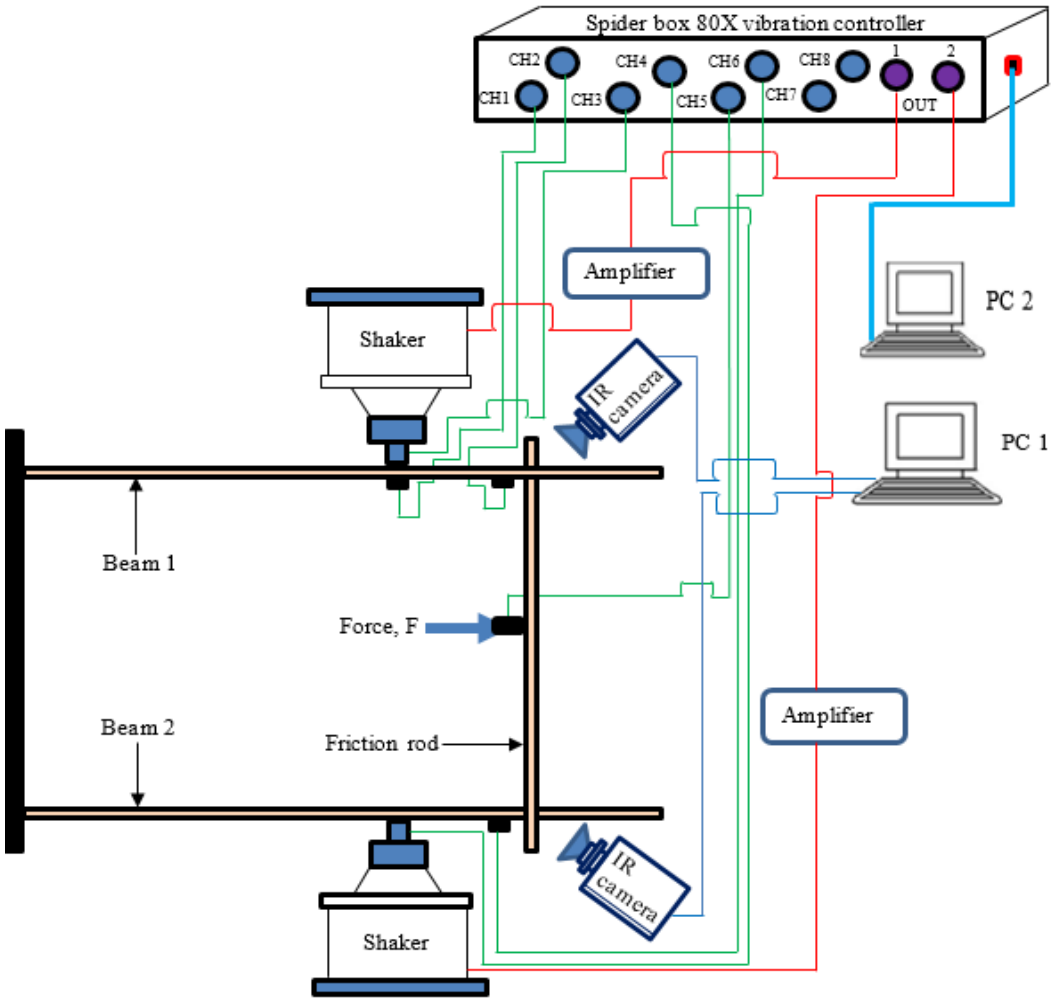

Fig. 2. Laboratory experimental setup.

4. Results and Discussions

The generated displacement or frictional temperature evolution time domain does not seem, by eye, to have any underlying sinusoidal signal components, instead it seems completely random and consisting of noise. However, the Discrete Fourier Transform (DFT) analysis checks for the spectral peak. The DFT for a sequence, $x(nT)$, is given by

$$\boldsymbol{X(kF) = \sum_{n=0}^{N-1} x(nT) e^{-j2\pi kFnt}} \quad (7)$$

where N is the number of samples, F is the spacing of frequency domain samples, T is the sample period in the time domain, k and n are integers. Fortunately, the MATLAB Fast Fourier Transform (FFT) function performs computation of DFT in an efficient way, hence, utilised in this study for the frequency analysis.

Therefore, this section, firstly analysed the frequencies and displacement from data acquired using the described accelerometer

sensors. Also, both displacement and interface lateral force statistics for the purpose of understanding the dispersion behaviour are presented. Secondly, analysed frequencies and displacement from the respective thermal imaging. Thanks to the IR camera temperature time-domain enhancement. The post analysis of thermal imaging hottest point yields the temperature time-history for the entire experimental period, hence, facilitating the structural frequency extraction. Furthermore, the developed transverse displacement analytical model Eq. (6) was utilised through incorporation of the greatest interface lateral force and interface finite temperature distribution as per Eq. (2) measured in the respective thermal imagers as considered in sub-sections 4.1 and 4.2, including the ambient recorded temperature during the experiments (22.4 ℃).

4.1 Excitation of both beams at 20 Hz

The accelerometer sensor measured response showed both beams to oscillate at 20.0401 *Hz* (Fig. 3). The displacement statistics indicated beam 1 with greater variation as seen with the large standard deviation that was attributed to the dynamics emanating from the beams excitations (Table 3).

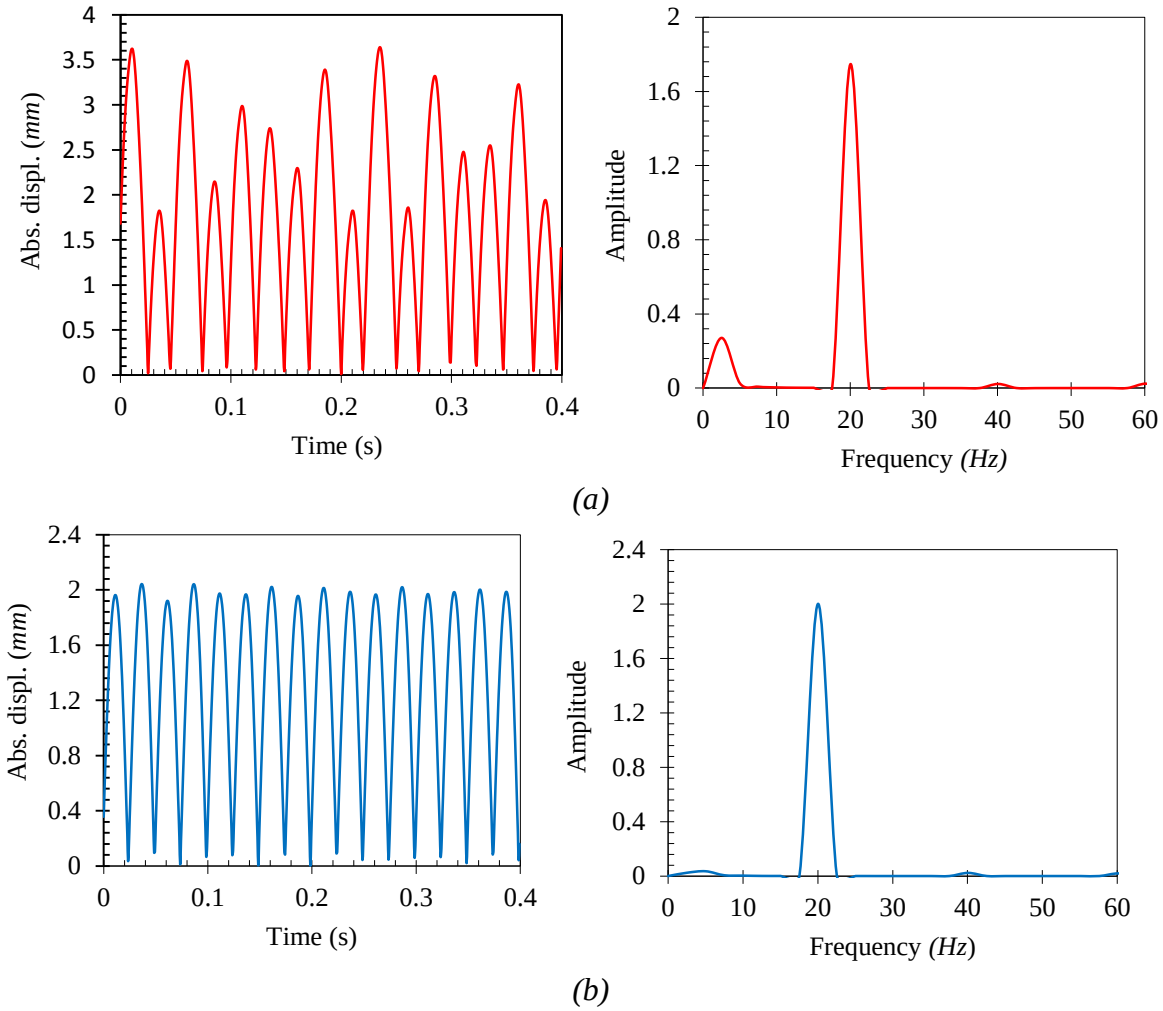

Fig. 3. Displacement time domain and FFT for both beams excited at 20 *Hz (a) beam 1 and (b) beam 2.*

Table 3 Displacement statistics (both beams excited at 20 Hz)

	Displacement (mm)		Interface force (N)
Description	Beam 1: 20 Hz	Beam 2: 20 Hz	
Mean	1.760	1.276	10.38
Max.	3.641	2.043	12.39
Min.	0.010	0.002	8.97
Range	3.630	2.040	3.42
Std. deviation	0.966	0.613	1.02

The analysis of thermal imaging of Fig. 4, analysed the structural frequencies to be 19.9885 Hz (Fig. 5a) and 19.9973 Hz (Fig. 5b) for beam 1 and 2, respectively. These were in good agreement with those measured using accelerometer (Fig. 3) with relative difference being 0.26 % and 0.21 % for beam 1 and beam 2, respectively. Further, beam 1 possessed several smaller frequencies that were associated with the beam multi-dynamics emanating from the periodic loading.

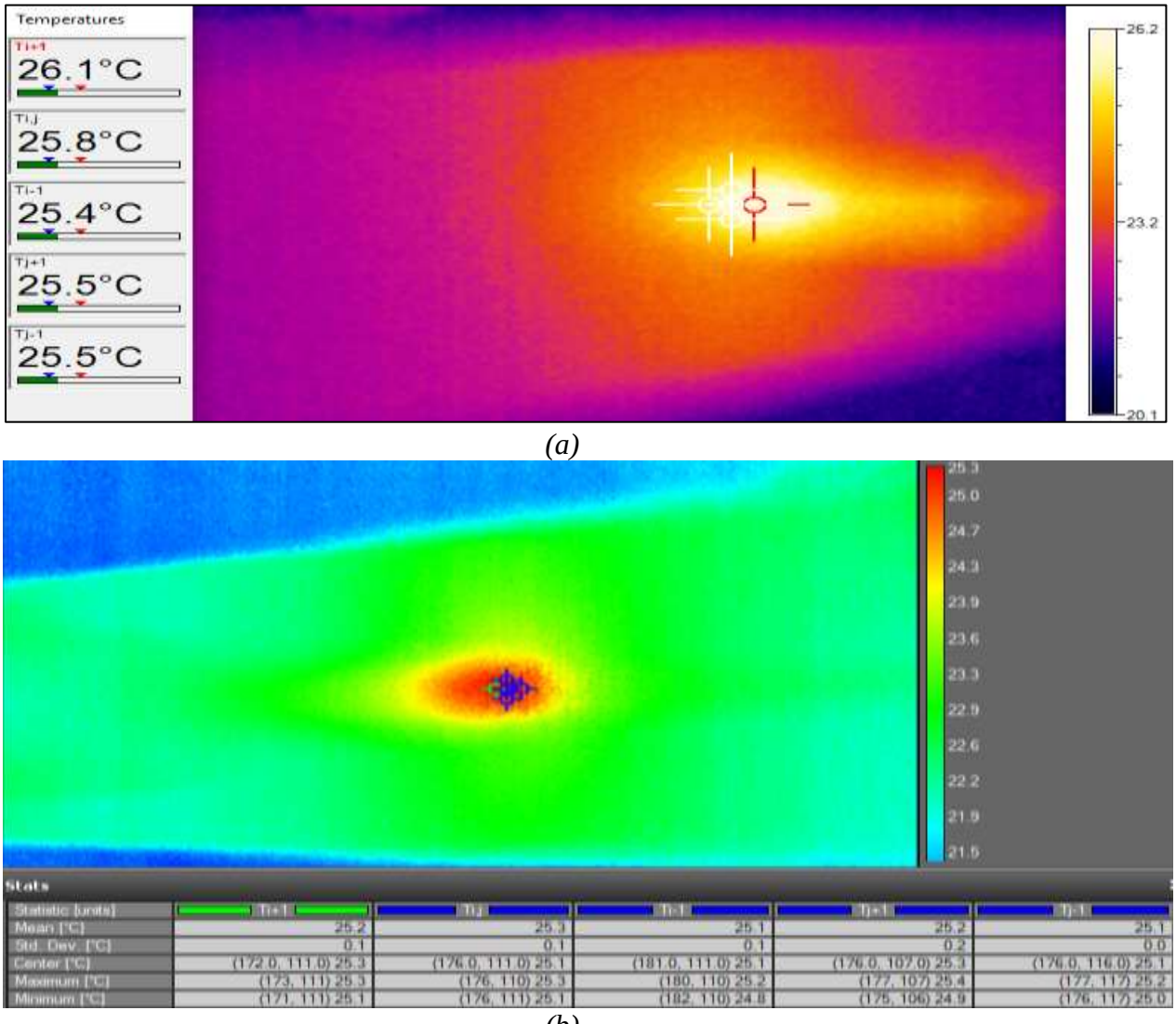

(a)

(b)

Fig. 4. Thermal images after 150 s for both beams excited at 20 Hz *(a) beam 1 and (b) beam 2*.

The interfacial lateral force on each beam measured 6.195 N (Table 3). Consequently, in the analysis of the displacement based on the thermal imaging for beam 1 (Fig. 4a); the

interface finite temperature along X direction was obtained as $-0.1\,℃/mm^2$, along Y direction as $-0.6\,℃/mm^2$ and transverse displacement as $1.748\,sin(\omega t)\,mm$. Likewise, in the case of beam 2 (Fig. 4b); the finite temperature along X direction evaluated as $-0.3\,℃/mm^2$, along Y direction as $-0.3\,℃/mm^2$ and the transverse displacement obtained as $1.491\,sin(\omega t)\,mm$. Compared to the accelerometer measured mean displacement (Table 3), the relative differences were 0.68 % and 14.42 % for beam 1 and beam 2, respectively.

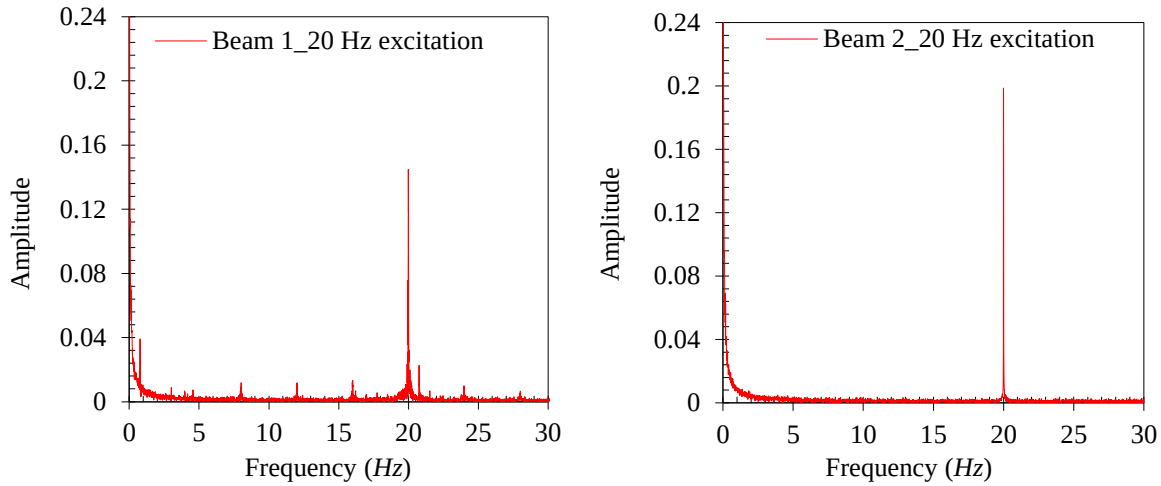

(a) *(b)*

Fig. 5. FFT of temperature evolution for both beams excited at 20 *Hz (a) beam 1 and (b) beam 2.*

4.2 Excitation of beam 1 at 40 Hz and 20 Hz

The accelerometer sensor displacement analysis indicated beam 1 oscillated at 40.0802 Hz (Fig. 6a), while beam 2 at 20.0401Hz (Fig. 6b). The excitation at 40 Hz resulted in displacement of lower mean compared to that of 20 Hz in addition to being closely distributed as seen with a smaller standard deviation in Table 4.

When the frictional force moves through a certain distance, a given amount of heat energy is dissipated. The first law of thermodynamics state that, at equilibrium, the energy into a system equals the sum of the energy accumulated and the energy output to the environment [18].

$$\boldsymbol{E_{system} = E_{accumulated} + E_{lost}} \quad (8)$$

The friction power input is the product of the frictional force F and the sliding speed v. Mabrouki et al. [8] reported that frictional energy consumed or stored in the material as micro-structural changes such as dislocations and phase transformation in general is about 5 %. The remaining part of the frictional energy raises the interface temperature. Further, Montanini and Freni [10] explained that the amount of frictional heat generated depends on several parameters, which includes coefficient of friction, normal applied force and the sliding relative speed.

However, since this study kept other factors constant while the excitation frequency varied. As expected, frictional heat increased for beam excited at 40 Hz compared to that at 20 Hz as evidenced by the results of thermal imaging results, where significant large temperature difference of 3.2 ℃ (Fig. 7) was observed. Moreover, Mabrouki et al. [8] observed similar findings on investigation of the frictional heating model for efficient use of vibrothermography. Hence, the conclusion was that frictional heat increases with the interface frequency.

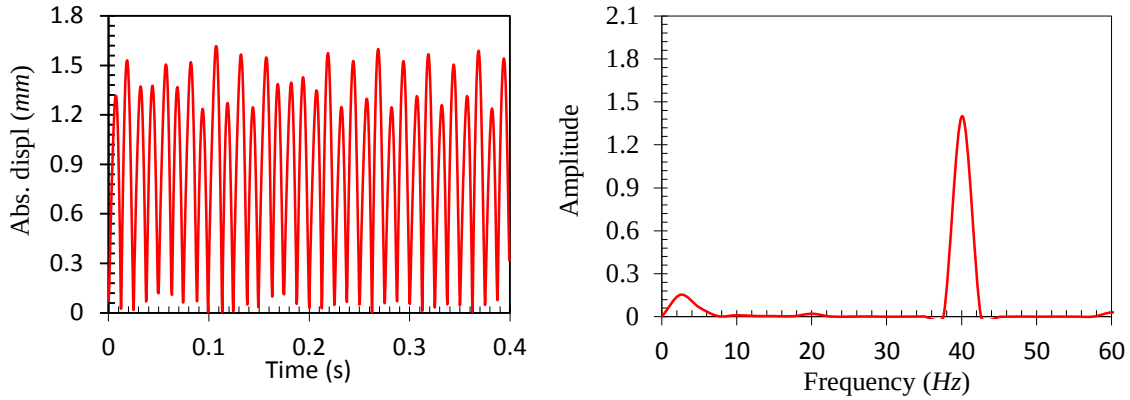

(a)

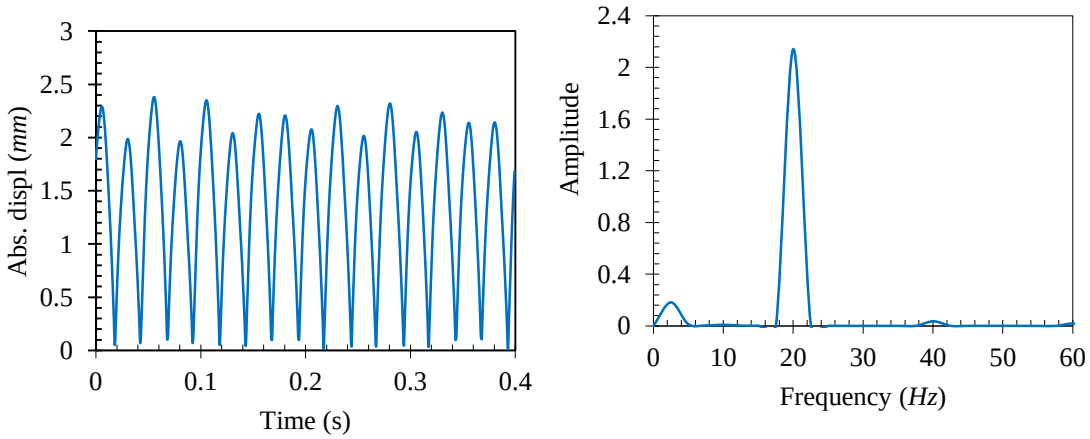

(b)

Fig. 6. Displacement time domain and FFT for *(a) beam 1: 40 Hz and (b) beam 2: 20 Hz.*

Table 4
Displacement and interface force statistics *(beam 1: 40 Hz and beam 2: 20 Hz)*

	Displacement (mm)		Interface force (N)
Description	Beam 1: 40 Hz	Beam 2: 20 Hz	
Mean	0.894	1.372	24.15
Max	1.616	2.381	27.52
Min	0.004	0.015	19.23
Range	1.612	2.366	8.29
Std. deviation	0.450	0.655	2.48

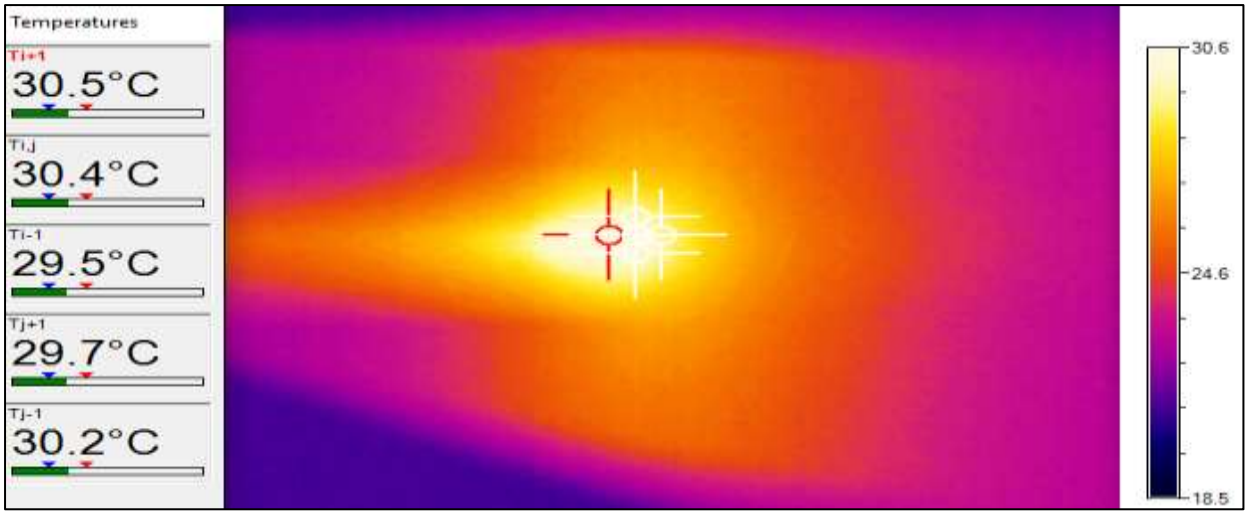

(a)

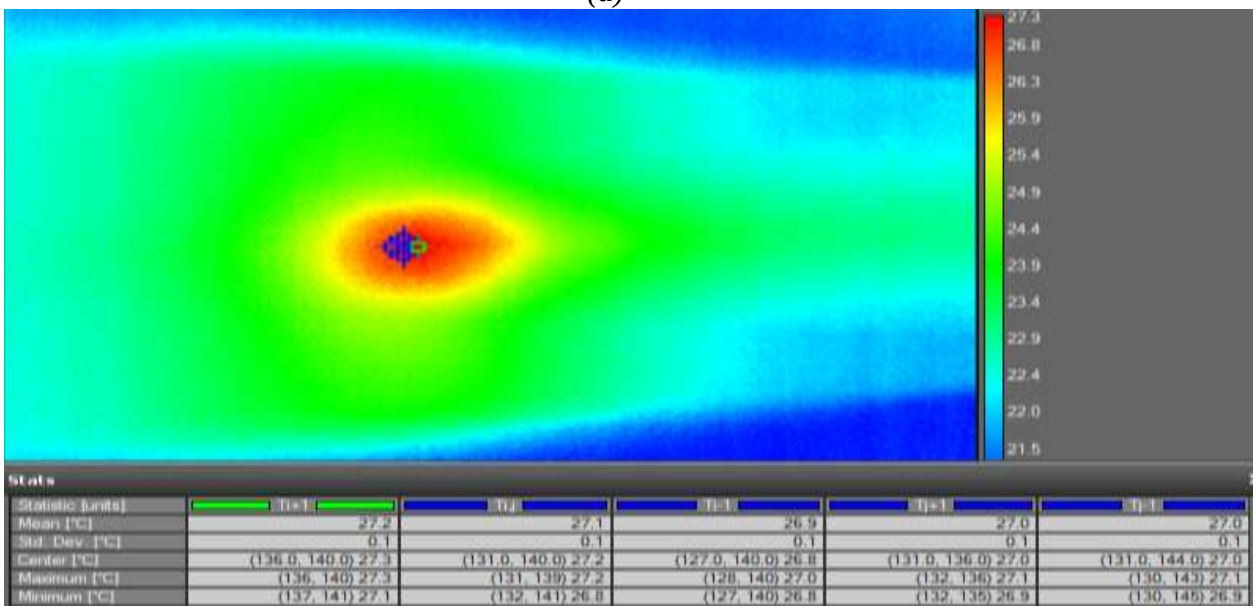

(b)

Fig. 7. Thermal imaging after 150 *s* for *(a) beam 1 at 40 Hz and (b) beam 2 at 20 Hz*.

The frequencies analysed from thermal images were 39.9686 *Hz* (Fig. 8a) and 20.00 *Hz* (Fig. 8b) for beam 1 and beam 2, respectively. Compared to the accelerometer sensor measured frequencies, relative differences were 0.28 % and 0.20 % for the former and latter, respectively.

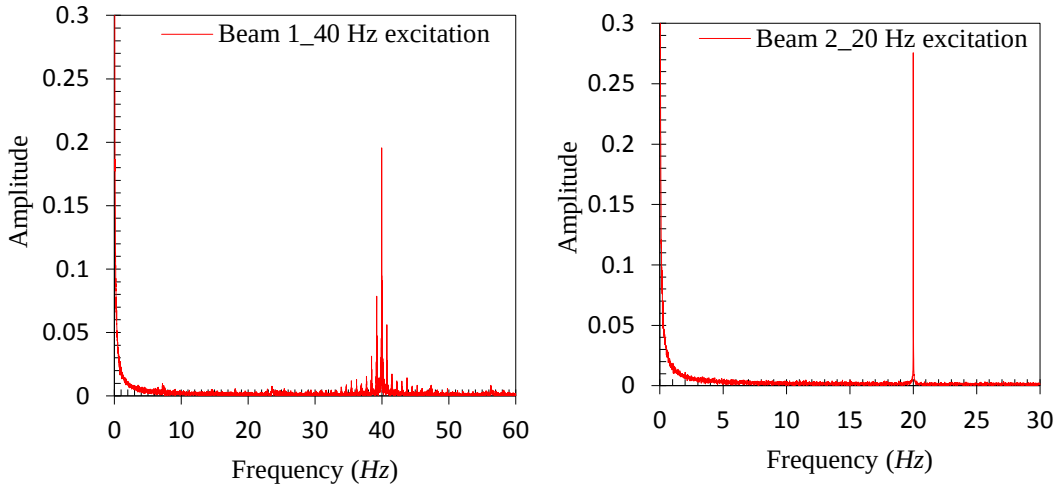

(a) *(b)*

Fig. 8. FFT of temperature evolution *(a) beam 1 at 40 Hz and (b) beam 2 at 20 Hz.*

The interfacial lateral force on each beam measured 13.7 $\boldsymbol{N}$ (Table 4). In the analysis of the displacement based on thermal imaging for beam 1 (Fig. 7a); the interface finite temperature along $\boldsymbol{X}$ direction obtained as $-\mathbf{0.8}\,℃/\boldsymbol{mm^2}$, along $\boldsymbol{Y}$ direction as $-\mathbf{0.9}\,℃/\boldsymbol{mm^2}$ and the displacement as $\mathbf{0.9258}\,\boldsymbol{sin(\omega t)}\,\boldsymbol{mm}$. Similarly, in the case of beam 2 (Fig. 7b); the finite temperature along $\boldsymbol{X}$ direction obtained as $-\mathbf{0.1}\,℃/\boldsymbol{mm^2}$, along $\boldsymbol{Y}$ direction as $-\mathbf{0.2}\,℃/\boldsymbol{mm^2}$ and displacement computed as $\mathbf{1.0878}\,\boldsymbol{sin(\omega t)}\,\boldsymbol{mm}$. Likewise, displacement acquired from the analysis of thermal images generally agreed well with the mean displacements acquired using accelerometer (Table 4) with relative differences being 3.43 % and 20.71 % for beam 1 and beam 2, respectively.

5. Conclusion

In this paper, the adequacy of monitoring structural vibration characteristics using Infrared Thermography for beam-like structures has been studied experimentally. IRT predicted frequencies were in good agreement with those from miniature accelerometer sensors, the relative errors being 0.26 (beam 1) and 0.21 (beam 2) for both beams excited at 20 Hz, while being 0.28 (beam 1) and 0.20 % (beam 2) for the beam 1 excited at 40 Hz and beam 2 at 20 Hz. However, the displacements were 0.68 (beam 1) and 14.42 (beam 2) for both beams excited at 20 Hz, while being 3.43 % (beam 1) and 20.71 % (beam 2) for beam 1 excited at 40 Hz and beam 2 at 20 Hz, respectively. This difference is attributed to the use of coefficient friction and coefficient of convective heat loss from the literature which was not the real values as in the case of experiments.

Therefore, the overall conclusion was that Infrared Thermography is capable of reliably predicting structural vibration behaviour in terms of frequency and displacement as shown by the findings of this research work.

Acknowledgement

The authors greatly appreciate the support of Tshwane University of Technology, University of Pretoria and Eskom Power Plant Institute (South Africa) in funding this research.

References

[1]. S. Saxena, J. P. Pandey, R. S. Solanki, G. K. Gupta,O. P. Modi, Coupled mechanical, metallurgical and FEM based failure investigation of steam turbine blade. Engineering Failure Analysis, 52 (2015) 35-44.

[2]. A. J. Oberholster, P. S. Heyns, Online condition monitoring of axial-flow turbomachinery blades using rotor-axial Eulerian laser Doppler vibrometry. Mechanical Systems and Signal Processing, 23 (2009) 1634-1643.

[3]. N. K. Mukhopadhyay, S. G. Chowdhury, G. Das, I. Chattoraj, S. K. Das, D. K. Bhattacharya, An investigation of the failure of low pressure steam turbine blades. Engineering failure analysis, 5 (1998) 181-193.

[4]. F. Wei, Q. Pizhong, Vibration-based Damage Identification Methods: A Review and Comparative Study. Structural Health Monitoring, 10 (2010) 83-111.

[5]. M. S. E. Torshizi, Y. S. M. Nikravesh, A. Jahangiri, Failure analysis of gas turbine generator cooling fan blades. Engineering Failure Analysis, 16 (2009) 1686-1695.

[6]. B. O Al-Bedoor, Discussion of the available methods for blade vibration measurement. In: ASME 2002 Pressure Vessels and Piping Conference. Vancouver, BC: Canada., 1561 (2002) 53-61.

[7]. J. Renshaw, J. C. Chen, S. D. Holland, T. R. Bruce, The sources of heat generation in vibrothermography. NDT & E International, 44 (2011) 736-739.

[8]. F. Mabrouki, M. Thomas, M. Genest, A. Fahr, Frictional heating model for efficient use of vibrothermography. NDT & E International, 42 (2009) 345-352.

[9]. B. B. Lahiri, S. Bagavathiappan, C. C. Soumya, V Mahendran, V. P. M Pillai, John P. J., T. Jayakumar, Infrared thermography based defect detection in ferromagnetic specimens using a low frequency alternating magnetic field. Infrared Physics & Technology, 64 (2014) 125-133.

[10]. R. Montanini, F. Freni, Correlation between vibrational mode shapes and viscoelastic heat generation in vibrothermography. NDT & E International, 58 (2013) 43-48.

[11]. M. Singh, G. Lucas, Blade design & analysis for steam turbines. The McGraw-Hill Companies: United States of America, (2011) 20-60.

[12]. A. Guran, F. Pfeiffer, K. Popp, Dynamics with friction modelling, analysis and experiments. World scientific: Singapore (2001) 20-80.

[13]. G. Straffelini, Friction and Wear: Methologies for design and control. Springer: Trento, (2015) 21-58.

[14]. A. D Dimarogonas, S. A Paipetis,T. G Chondros, Analytical Methods in Rotor Dynamics (second edition) New York London: Springer Dordrecht Heidelberg: , (2013).

[15]. S. Bagavathiappan, B. B. Lahiri, T. Saravanan, J. Philip, T. Jayakumar, Infrared thermography for condition monitoring – A review. Infrared Physics & Technology, 60 (2013) 35-55.

[16]. A. D. Dimarogonas, N. B. Syrimbeis, Thermal signatures of vibrating rectangular plates. Journal of Sound and Vibration, 157 (1992) 467-476.

[17]. D. Thorby, Structural dynamics and vibration in practice: An engineering handbook. London: Elsevier Science, (2008) 45-60.

[18]. R. K. Rajput, Heat and Mass Transfer. S. Chard & Company Ltd, (2006) 30-40.

[19]. S. F. Miller, A. J. Shih, Thermo-Mechanical Finite Element Modeling of the Friction Drilling Process. Journal of manufacturing science and engineering, 129 (2007) 531-538.

[20]. C. F Beards, Structural vibration: Analysis and damping. London: Elsevier Science, (2003) 200-210.

[21]. W. P. Sanders, Turbine steam path engineering for operations and maintenance staff (first edition). Richmond Hill, Ontario: Canada, (1996) 236-239.

[22]. C. V. Madhusudana, Thermal conductance of cylindrical joints. International Journal of Heat and Mass Transfer, 42 (1999) 1273-1287.

[23]. J. T. Oden, J. A. Martins, Models and computational methods for dynamic friction phenomena. Computer methods in applied mechanics and engineering, 52 (1985) 527-634.